Science of the Total Environment 916 (2024) 170030

Contents lists available at ScienceDirect

Science of the Total Environment

journal homepage: www.elsevier.com/locate/scitotenv

Pyrene and its derivatives increase lung adverse effects by activating aryl hydrocarbon receptor transcription

Mei Wang [1], Na Luo [1], Yanpeng Gao, Guiying Li, Taicheng An [*]

Guangdong-Hong Kong-Macao Joint Laboratory for Contaminants Exposure and Health, Guangdong Key Laboratory of Environmental Catalysis and Health Risk Control, Institute of Environmental Health and Pollution control, Guangdong University of Technology, Guangzhou 510006, China
Guangzhou Key Laboratory of Environmental Catalysis and Pollution Control, Key Laboratory of City Cluster Environmental Safety and Green Development of the Ministry of Education, School of Environmental Science and Engineering, Guangdong University of Technology, Guangzhou 510006, China

HIGHLIGHTS

- Injury mechanism of pyrene derivatives on lung were explained *in vivo* and *in vitro*.
- Pyrene derivatives can activate AhR, causing adverse effects on the lungs.
- Binding energy and conformation of pyrene derivatives affect the expression of AhR.
- Pyrene derivatives could impose more serious risks on human lungs cells.

GRAPHICAL ABSTRACT

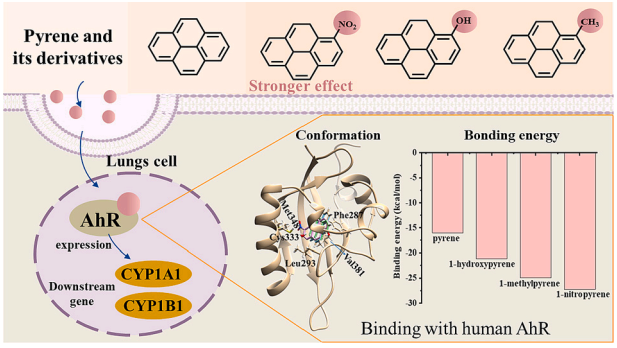

ARTICLE INFO

Editor: Lingyan Zhu

Keywords:
PAH derivatives
Aryl hydrocarbon receptor
Binding reactions
AhR activation
Molecular dynamics simulation
Adverse effects

ABSTRACT

Derivatives of polycyclic aromatic hydrocarbons (PAHs) pose significant threat to environment and human health due to their widespread and potential hazards. However, adverse effects and action mechanisms of PAH derivatives on human health have not been attempted yet. Herein, we chose pyrene and its derivatives (1-hydroxypyrene, 1-nitropyrene, and 1-methylpyrene) to investigate adverse effect mechanism to human lungs using *in vitro* and *in vivo* methods. Results showed that pyrene derivatives have higher lung health risks than original pyrene. They can activate AhR, subsequently affecting expression of downstream target genes CYP1A1 and CYP1B1. The binding energies of pyrene and its derivatives ranged from −16.07 to −27.25 kcal/mol by molecular dynamics simulations, implying that pyrene and its derivatives acted as agonists of AhR and increased adverse effects on lungs. Specifically, 1-nitropyrene exhibited stabler binding conformation and stronger AhR expression. In addition, sensitivity of pyrene and its derivatives to AhR activation was attributed to type and number of key amino acids in AhR, that is, pyrene (Leu293), 1-nitropyrene (Cys333, Met348, and Val381), 1-hydroxypyrene (Leu293 and Phe287), and 1-methylpyrene (Met348). In summary, we provide a universal

* Corresponding author at: Guangzhou Key Laboratory of Environmental Catalysis and Pollution Control, Key Laboratory of City Cluster Environmental Safety and Green Development of the Ministry of Education, School of Environmental Science and Engineering, Guangdong University of Technology, Guangzhou 510006, China.
E-mail address: antc99@gdut.edu.cn (T. An).
[1] These authors contributed equally to this work and were considered as co-first authors.

https://doi.org/10.1016/j.scitotenv.2024.170030
Received 22 September 2023; Received in revised form 27 December 2023; Accepted 7 January 2024
Available online 12 January 2024

approach for understanding action mechanisms of PAH derivatives on human health, and their adverse effects should be taken seriously.

1. Introduction

Polycyclic aromatic hydrocarbons (PAHs) and their derivatives are widespread environmental pollutants. Compared to PAHs, its derivatives exhibit more accumulative in biotas and a higher tendency for spreading from contaminated sites (Jin et al., 2023). Especially hydroxyl-, nitro- and methyl-PAH derivatives are of increased concern and they have been widely detected in environmental media (Mueller et al., 2019), including atmosphere (Li et al., 2022; Zhang et al., 2022b), soil (Idowu et al., 2020), sediments (Han et al., 2019) and water (Mohammed et al., 2021). Noteworthy, PAH derivatives are reported to be much more toxic than PAHs, although the concentration of several derivatives is approximately 1–3 orders of magnitude lower than parent PAHs (Huang et al., 2014; Tomaz et al., 2016). These PAH derivatives could cause significant toxic effects. Nitro-PAHs are considered as direct mutagens (Misaki et al., 2016) and strong carcinogens especially on lung cancer metastasis (Gao et al., 2019). Additionally, nitro-PAH exposure induces inflammatory responses in human lungs cells (Hu et al., 2020), listed as probable human carcinogens by the International Agency for Research on Cancer (IARC) (Li et al., 2020). Exposure to hydroxyl-PAHs can also induce the formation of protein adducts PAH-DNA, affecting the normal activity of proteins (Berge et al., 2004) and alter promoter methylation (Motorykin et al., 2015), including 1-hydroxypyene positively correlated with oxidative inflammatory markers and myocardial infarction (Freitas et al., 2014). There is limited knowledge on the developmental toxicity for the methyl-PAHs. The activation of human aryl hydrocarbon receptor (AhR) by methylated PAHs is two to five times stronger than that of the parent PAHs (Sun et al., 2014). In addition, methylated PAHs may alter its developmental toxicity (Fang et al., 2022). Therefore, these PAH derivatives could impose health risks and it is critical to understand their toxicity mechanisms.

It is believed that the adverse effects of PAHs is linked with the activate the signal transduction pathway of AhR (Vondracek et al., 2017). After entering the cell, PAHs can first bind to AhR, triggering the adverse effect (Jin et al., 2018). This interaction between PAHs and AhR not only determines the agonistic potential of PAHs, but also distinguishes differences in AhR across animal studies. For instance, 2,3,7,8-tetrachlorodibenzo-*p*-dioxin (TCDD), which binds to the ligand-binding domain of AhR, was generally considered a potent exogenous agonist of AhR except for its toxic effects on frogs and toads (Shoots et al., 2015). Binding of dioxin-like compounds to AhR could be utilized to determine the differences in sensitivity between white and lake sturgeon (Doering et al., 2015). Moreover, the activation of dioxins and their analogues through different interaction modes with AhR could serve as a predictive method for detecting environmental risk assessment (Hwang et al., 2020). However, the controversy in human studies regarding AhR activation by PAHs mainly concerns the specific types of PAHs involved. Many abundant six-ring PAHs are relatively potent AhR agonists in human lung cells (Vondracek et al., 2020), while certain low-ring PAHs exhibit activation and antagonism pathways towards AhR in different human cell types. For instance, exposure to low doses of pyrene resulted in minor changes to AhR-regulated gene expression in human hepatocytes (Luo et al., 2022). On the contrary, pyrene acted as an antagonist for AhR-induced genes in human microvascular endothelial cells (Brinchmann et al., 2018). What's more, most PAHs including naphthalene and phenanthrene are not agonists of AhR, but their hydroxylated or alkylated derivatives are potent agonists (Lille-Langoy et al., 2021). Moreover, PAH derivatives with AhR action patterns in human health are rarely studied.

In this work, we conducted *in vitro* and *in vivo* studies on the AhR signaling pathway induced by typical PAH (pyrene) and its derivatives (1-hydroxypyrene, 1-nitropyrene, and 1-methylpyrene). Western Blot assay was employed to detect the expression of AhR protein under exposure to PAHs and its derivatives. Quantitative real-time PCR (qPCR) was utilized to evaluate the action effect on AhR by detecting the expression of AhR target genes CYP1A1 and CYP1B1. Furthermore, molecular dynamics (MD) simulations were performed to investigate the molecular initiation events between four pyrene compounds and the ligand binding domain of AhR (AhR LBD), aiming to identify potential AhR agonists among pyrene derivatives. Finally, trajectory analysis module and molecular mechanics energy analysis in MD simulations were employed to elucidate the role of key amino acid residues. Our study provides evidence at the molecular and atomic levels of differentially activated AhR levels and mechanisms of adverse effects of pyrene and its derivatives on the lung.

2. Methods

2.1. Chemicals and reagents

Pyrene (97 %) and 1-nitropyrene (98 %) were from Maclin (Shanghai, China), 1-hydroxypyrene (98 %) were purchased from Aladdin (Shanghai, China), 1-methylpyrene and 3,3′,4,4′,5-pentachlorobipheny (PCB 126) was purchased from Beijing Bellingwei Technology Co., LTD. DEME culture medium, fetal bovine serum (FBS), penicillin-streptomycin and trypsin-EDTA for cell culture were purchased from Thermo Fisher Scientific, dimethyl sulfoxide (DMSO, >99 %) was obtained from Aladdin, phosphate buffer was purchased from Bioengineering (Shanghai, China), and the kits for extraction of cell nuclear and cytoplasmic proteins and BCA protein concentration determination were purchased from Shanghai Beyotime. AhR antibody (rabbit monoclonal antibody), β-actin antibody (rabbit monoclonal antibody) and Lamin B1 antibody (rabbit monoclonal antibody) were purchased from Cell Signaling Technology, Trizol reagent was obtained from Thermo Fisher Scientific. Premix and De-genomic and Reverse Transcription Triple Premix were purchased from Mona.

2.2. Cell culture, RNA extraction, qPCR and Western Blot

The cells used were human bronchial epithelial cells (16HBE), which were provided by the General Hospital of Guangzhou Military Region. 16HBE cells were sown in DMEM medium supplemented with 1 % penicillin-streptomycin and 10 % fetal bovine serum and grown at 37 °C in a 5 % CO_2 incubator. Pyrene and its derivatives were dissolved in DMSO, with the final cell exposure containing little >1 ‰ DMSO.

Total RNA was extracted from 16HBE cells with Trizol reagent and quantified using a NanoDrop one ultra-micro spectrophotometer (Thermo Fisher Scientific) using MonScriptTM RTlll All-in-One Mix with dsDNase kit to obtain cDNA template. The qPCR assay was performed in a Bio-Rad CFX instrument using the MonAmpTM ChemoHS qPCR Mix kit. The β-actin was used as an internal reference.

To extract total proteins, cold cells were lysed using Ripa cell lysate. Cold cells' nucleus and cytoplasm proteins were extracted separately using nucleus and cytoplasm protein extraction kits. BCA protein assay was used to quantify total protein content. The β-actin was used as an internal reference for cytoplasm-extracted proteins, and Lamin B1 was used as an internal reference for nucleus-extracted proteins. Equal amounts of proteins were transferred to nitrocellulose membranes after being separated by the electrophoresis solution gel, and the membranes were blocked with 5 % skimmed milk powder in PBS-T (1 ‰) configuration, and then the nitrocellulose membranes were incubated with diluted antibody (1000:1) overnight at 4 °C.

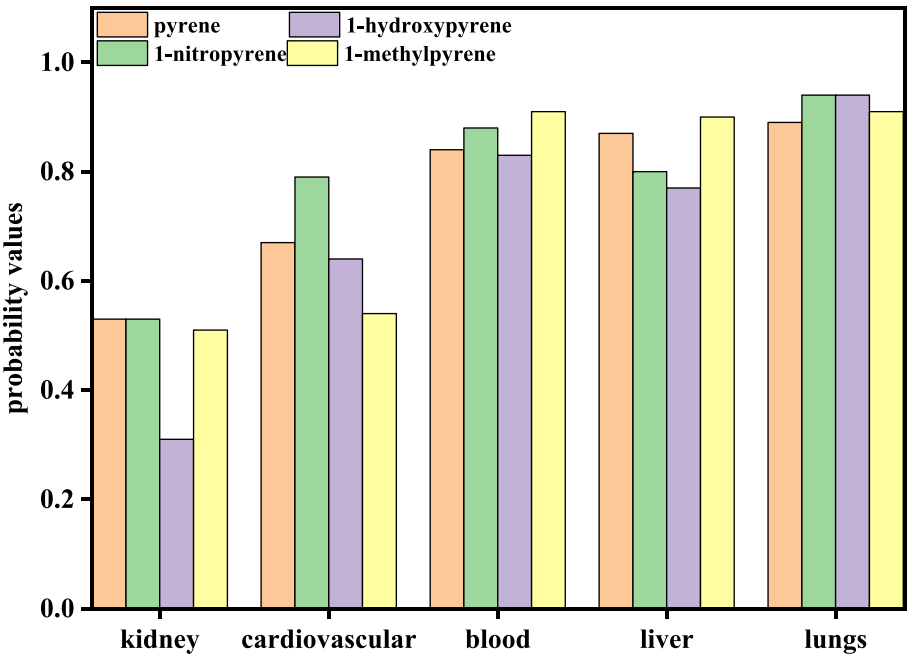

Fig. 1. Predictive value of adverse effects of pyrene and its derivatives on human organ.

After washing three times using PBS-T (1 ‰), the secondary antibody was incubated at room temperature for 2 h and the membrane was washed three more times with PBS-T (1 ‰). The protein bands were then detected by Tanon.

2.3. Computational the probability of health effect

The ACD/Percepta platform's Health Effects module (ACD/labs, 2016) was utilized to predict probabilities of organ-specific adverse effects on pyrene and three derivatives, including kidney, cardiovascular, blood, liver and lungs. This module has demonstrated its efficacy in predicting the probability of organ-specific adverse effects within the therapeutic dose range (Gao et al., 2023; Gawlik et al., 2020). The predict values for the probability of adverse effects on humans, pertaining to pyrene and its derivatives, are based on the data for >100,000 compounds collected from chronic, subchronic, acute toxicity and carcinogenicity studies with adverse effects reported on particular organs or organ systems. Through the known chemical structure, the corresponding prediction results are obtained. The predicted probability values range from 0 to 1, with a closer approach to 1 indicating a more significant adverse effect on the organ.

2.4. Homologous modeling

The three-dimensional structure of AhR generated from humans and its ligand complexes has yet to be established. The structural information of the AhR Per-Arnt-Sim (PAS) B ligand-containing binding domain has not been reported to be experimentally determined, so a reliable model of the human AhR PAS B structural domain was established using comparative modeling techniques using the extensive structural information of the homologous PAS-containing protein. To create models with the greatest sequence homology and resemblance to AhR, the PAS structural domains of functionally related hypoxia-inducible factor 2α (HIF-2α) and AhR nuclear translocation (ARNT) proteins were chosen. As a result, Models for LBD of AhR were generated by use of Modeler 9.21 (University of California, San Francisco, CA) run through Easy-Modeller 4.0 (Kuntal et al., 2010), selecting the NCBI sequence number AAH70080.1 of human AhR (https://www.ncbi.nlm.nih.gov/protein/7304873), summarizing previous studies, modeling proteins with PAS structural domains of HIF-2α and ARNT proteins from the RCSB protein database (PDB ID: 1p97, 3h82, and 3h7w) (Hirano et al., 2015), and amino acid sequences ranging from 274 to 390 as target template. After performing a BLAST sequence comparison, the templates with the highest scores were chosen for multi-template building, the sequences of the key ligand domains are at 278–390. Programs such as Ramachandran plot, ProSA z-scores (Wiederstein and Sippl, 2007) and the Computed Atlas of Surface Topography of Proteins (CASTp) (Dundas et al., 2006) server were evaluated separately for the built templates to enable the model to perform docking simulations.

2.5. Molecular docking

The ligand structures in the computational analysis were downloaded from PubChem (https://pubchem.ncbi.nlm.nih.gov/) and optimized with Gaussian 09 (base group B3LYP/6–311++G(d,p)) prior to ligand docking (Frisch et al., 2013). To examine the bioactive conformations of PAHs and their hydroxyl, nitro, and methyl pyrene derivatives and to model their probable interactions in the binding pocket of AhR, we used AutoDock 4.0 to conduct protein-ligand docking simulations (Morris et al., 2009). Polar hydrogens were added using the AutoDock Tools (ADT) 1.5.6 software with 60 docking runs using the Lamarck Genetic Algorithm with default settings, a very effective approach for modeling and visualizing ligand-protein complexes in three dimensions. The average of the free energy displacements of each ligand in the AhR docking site simulation was used to determine the ligand binding energy U_dock. The protein-ligand interaction analyzer was used to predict the interactions of each substance with the AhR homology model's amino acid residues. PyMOL 1.8 was used to visualize the model (http://www.pymol.org).

2.6. MD simulation

GROMACS 2019.5 (Abraham et al., 2015) was utilized to perform MD simulations, which depict the dynamic interactions between atoms and molecules within a given system. Amber99SB force field was used for protein structures and GAFF force field was used for pyrene and derivatives (Zhang et al., 2022a). Protein-ligand complexes are solvated in boxes with TIP3P water molecules, keeping the boundaries of the box

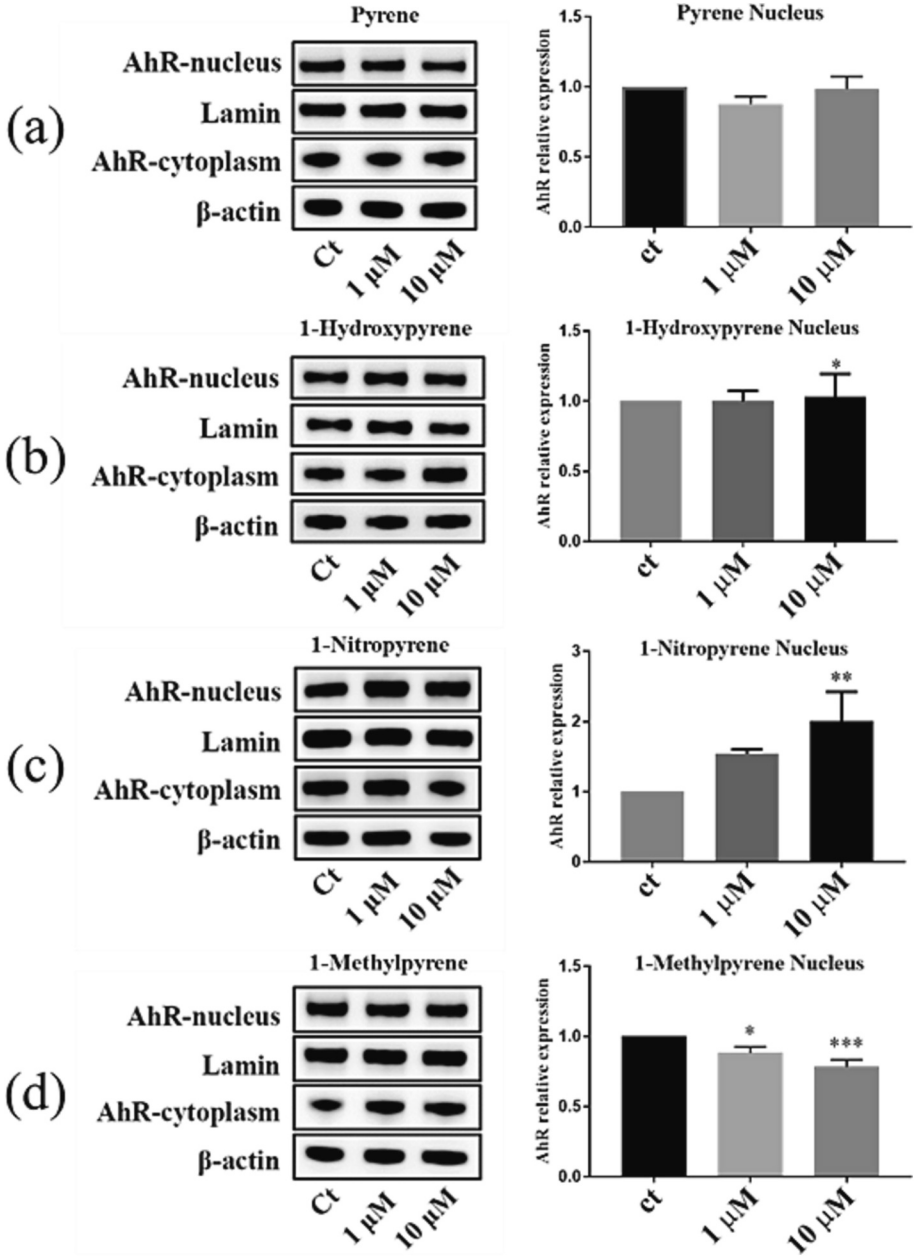

Fig. 2. AhR nucleus protein. 16HBE cells were treated with the test compounds for 48 h and whole cell lysates were analyzed by Western blots. Significant induction of AhR is indicated by (*).

at least 1 nm away from all protein atoms. Five chloride ions were subsequently added for charge neutralization. The entire system was then energy minimized using the most conjugate gradient method, which was gradually heated from 0 to 310.15 K at a constant volume. The heating system ligands were positional restricted and equilibrated for 1 ns at 1 bar and 310.15 K, after which MD simulations were performed in the NPT ensemble with periodic boundary conditions. Electrostatic and van der Waals interactions were calculated using the particle grid Ewald (PME) algorithm, and all simulations were performed with a time step of 2 fs for at least 40 ns, and snapshots for analysis were saved every 2 ps. Trajectories obtained from MD simulations were used for binding free energy calculations of the molecular mechanics Poisson−Boltzmann surface area (MM-PBSA) (Kumari et al., 2014). Molecular mechanical energy (E_{MM}) analysis was used to identify key amino acids. The root mean square deviation (RMSD) was used to analyze the system's mobility and convergence. To determine the stability of binding, we analyzed trajectories using the VMD 1.9.3 analytic tool (Humphrey et al., 1996).

3. Results and discussion

3.1. Health effects of pyrene and its derivatives

PAHs enter the human body through breathing, skin contact, dietary intake, and other means, affecting the normal functioning of organs such as the liver and kidneys, and even causing cancer (Gysel et al., 2018). However, the effects of pyrene and its derivatives on internal organs and potential health risks are still unclear. Therefore, the ACD/Percepta platform was utilized to computationally predict the adverse risks of pyrene and its derivatives on multiple organs, including the kidney, cardiovascular system, blood, liver, and lungs. The results are shown in Fig. 1. Herein, the probability (p) value between 0 and 1 was obtained for a test compound to predict the health effects. As the p value close to 1, the potential risk of the test compound is higher. As shown in Fig. 1,

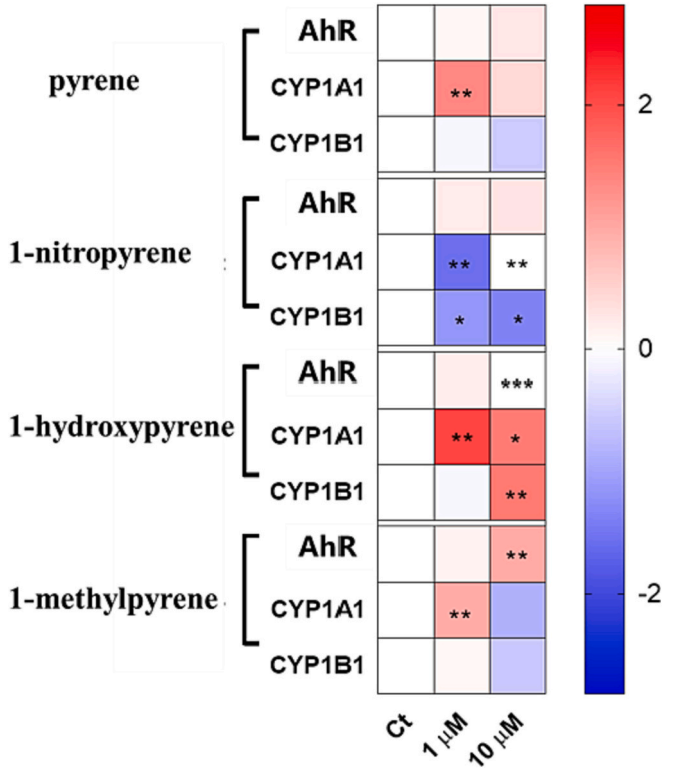

Fig. 3. A heat map of gene expression profiles generated using the average gene expression values of three biological replicates, with fold changes in gene expression given in cells. (see legend).

the highest *p* values of pyrene were 0.89 for lungs, followed by 0.84 for blood and 0.87 for liver. These data indicate that the lungs were the most vulnerable organ to adverse effects of pyrene. Moreover, the *p* values of its derivatives were 0.94, 0.94, and 0.91 for 1-nitropyrene, 1-hydroxypyrene, and 1-methylpyrene, respectively. All these data are higher than that of original pyrene (0.89), implying that the three derivatives could impose more serious risks on human lungs relative to pyrene. Furthermore, previous epidemiological and experimental observation also confirmed that exposure to derivative 1-nitropyrene can induce chronic obstructive pulmonary disease (COPD) (Li et al., 2017). Evidently, pyrene and its derivatives exert more pronounced adverse effects on the human lung, albeit with limited knowledge of their underlying mechanisms. Consequently, we conducted *in vitro* studies on the pulmonary effects of pyrene and its derivatives, utilizing health effect values as a basis, to elucidate the activation of AhR by these compounds and thereby assess their associated health risks to humans.

3.2. Transcriptional activation of pyrene and its derivatives towards AhR

Generally, AhR plays an important role in the adverse effects induced by PAHs. To investigate the adverse effects of pyrene derivatives on lung cells, we analyzed AhR transcription activated pyrene and its derivatives in 16HBE cells using western blot. Firstly, a well-known AhR agonist, PCB 126, was utilized to ensure the accuracy of experimental method. As depicted in Figs. S1 and S2, compared to the control group, exposure to PCB 126 exhibited 2.2-fold higher expression of AhR protein in the nucleus, further validating the reliability of the investigated approach. Subsequently, the expressions of AhR activated by pyrene and its derivatives were investigated and the results were presented in Fig. 2. Pyrene exposure did not significantly affect the expression of AhR protein (Fig. 2a), indicating that pyrene had a limited impact on AhR induction in lung cells. In contrast, exposure to the pyrene derivatives, 1-nitropyrene and 1-hydroxypyrene, could significantly increase the expression of AhR protein by 2 and 1.2 folds, respectively (Fig. 2b and c). Despite the estimated human exposure from atmospheric concentrations exhibiting a decreasing trend in the order of pyrene, 1-hydroxypyrene, and 1-nitropyrene, with the latter being approximately two orders of magnitude lower than pyrene (Hayakawa et al., 2020), noteworthy was the profound augmentation of AhR nuclear receptor expression at the protein level in 16HBE cells induced by pyrene derivatives, specifically 1-nitropyrene and 1-hydroxypyrene, thereby potentiating the detrimental impact on pulmonary health. While a decreasing trend was observed in the protein expression of 1-methylpyrene exposure (Fig. 2d), indicating that the adverse effects of derivative 1-methylpyrene on lung were different from the mechanism of 1-nitropyrene and 1-methylpyrene. Thus, it is necessary to determine the expression of AhR and AhR downstream genes induced by pyrene derivatives to estimate adverse effects on lungs.

In general, to assess the toxicity or carcinogenicity of exogenous compounds, it is necessary to determine the induction of AhR downstream genes (AhR, CYP1A1) (Garrison et al., 1996). To further verified the activation of AhR transcription by pyrene and its derivatives, the expression of AhR and its downstream target genes, CYP1A1 and CYP1B1 in human 16HBE cells were analyzed using qPCR assays (Fig. 3). Herein, the method was confirmed by the control PCB 126, and its mRNA expression was significant upregulation in AhR, CYP1A1, and CYP1B1 (Fig. S3). We further measured the expression of AhR and its downstream genes after 24 h exposure to pyrene and its derivatives at the concentration of 1 and 10 μM. As depicted in Fig. 3, we observed the upregulation of AhR gene expression after exposure to both pyrene and its derivatives, indicating that pyrene and its derivatives could induce the expression of downstream CYP enzymes. Accordingly, CYP1A1 was upregulated in response to pyrene exposure, while both CYP1A1 and CYP1B1 were upregulated in response to 1-hydroxypyrene exposure. Additionally, both CYP1A1 and CYP1B1 were expressed under exposure to 1-methylpyrene at a concentration of 1 μM. For 1-nitropyrene, no significant expressions were observed for CYP1A1 and CYP1B1. This is due to the fact that different ligands can mediate the expression of different CYP isoforms, which is related to enzyme-specific selection (Chai et al., 2021; Zhou et al., 2022). Taken together, these findings suggested that pyrene and its derivatives elicited signaling pathways that activate the AhR and induce different expression on downstream gene in 16HBE cells. Pyrene exhibited a weak interference on AhR activation, while 1-nitropyrene, 1-hydroxypyrene, and 1-methylpyrene demonstrated stronger activation effects than their parent compound. Therefore, it is necessary to constructe a human AhR model to explain the interaction mechanism of pyrene and its derivatives with AhR.

3.3. Homology models of human AhR LBD

The AhR model can be utilized to investigate the molecular-level differential activation expression of pyrene and its derivatives with human AhR. Unfortunately, no crystal structure of human AhR LBD has been determined experimentally as yet, and thus the 3-dimensional structure of the human AhR LBD should be constructed using homology modeling. The human AhR model was constructed based on the HIF-2α PAS-B domain due to its superior alignment with the AhR PAS-B sequence (Bisson et al., 2009). In addition, utilizing the HIF-2α structure as a template to improve the accuracy of binding site predictions (Wang et al., 2013; Zhang et al., 2018a). The obtained structure of the AhR LBD was shown in Fig. 4a and it consists of five β strands, a long central helix, and several small helices that are interconnected to naturally enclose the internal cavity. The reliability of this human AhR model was estimated using Ramachandran plot and ProSA server for validation. Ramachandran plot (Fig. 4b) showed that >90 % of amino acid residues fall in the most suitable region and no residue falls in the disallowed region. These indicate that the protein dihedral angles phi (Φ) and psi (Ψ) occupy fairly accurate positions for building the 3D model. ProSA z-score (Fig. 4c) showed that the *z*-score of AhR's ProSA

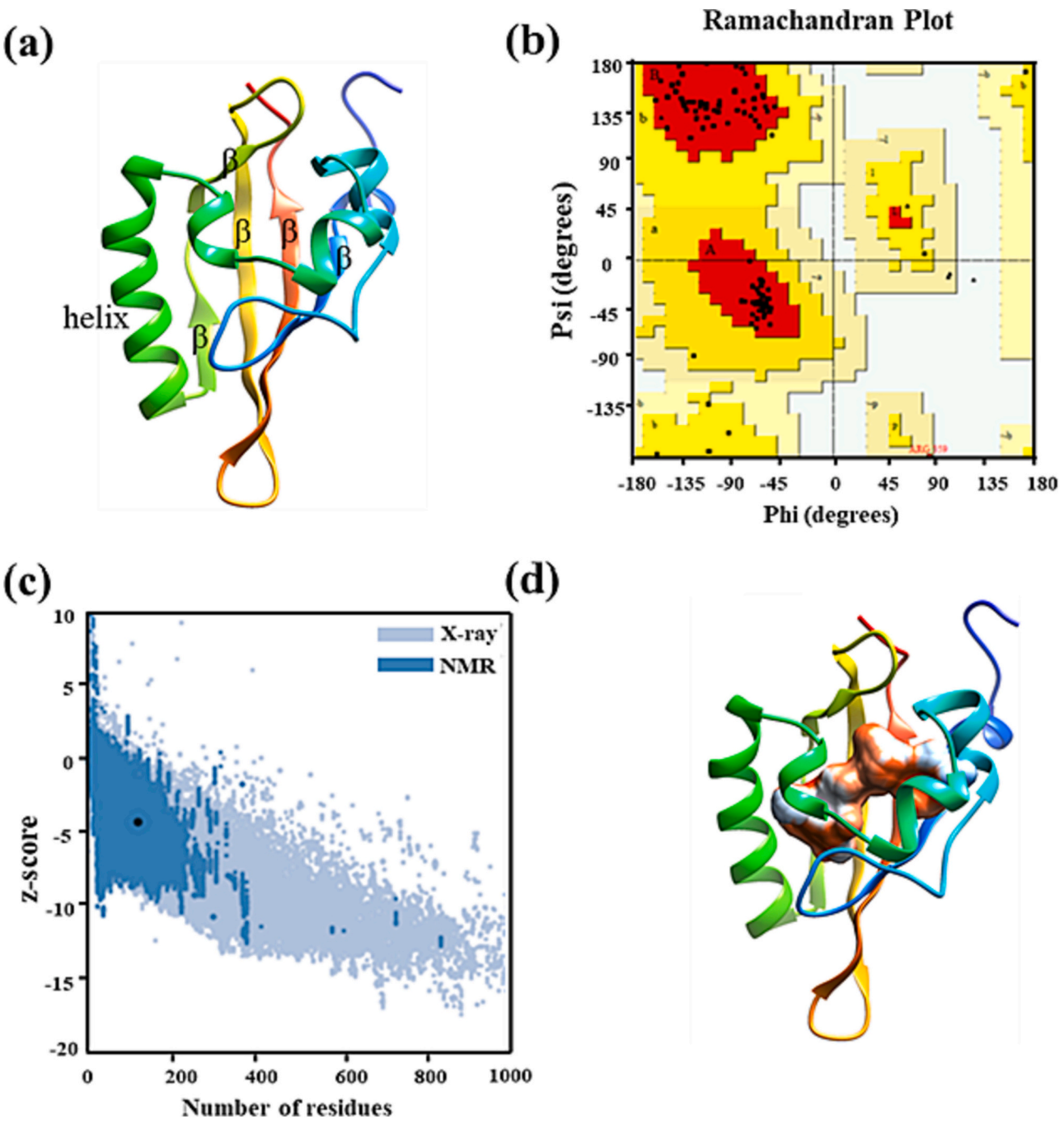

Fig. 4. (a) 3-D model of human AhR LBD structure. (b) Ramachandran plot, where Φ-Ψ torsional angles for all residues of AhR LBD were shown, and glycine residues were separately identified by triangles. The red areas represent the core regions and the most favorable combination of torsions, while yellow and light yellow represent the additionally and the generously favored areas respectively, and the rest white regions represent the disallowed areas. (c) Output from ProSA showing z-scores for models of AhR of human. (d) The red and white solid areas depict the molecular surface of the binding cavity identified by CASTp.

score is −4.32, which corresponds to the scoring interval of its protein counterpart (−3.51 to −4.54) (Pandini et al., 2007). Thus, both Ramachandran plot and ProSA *z*-score results confirmed the reliability of the constructed AhR template. From Fig. 4d, an internal cavity in the AhR LBD as a potential bioactive binding pocket for ligand capture was observed, and its size was calculated as 189 Å, which is fully available for pyrene and its derivative binding (< 9.8 Å). This large and deep hydrophobic cavity is favorable for binding of ligand pyrene derivatives with AhR protein, potentially resulting in the formation of protein-ligand complexes. Therefore, the effective binding interaction of AhR protein with pyrene and its derivatives deserved to be investigated.

3.4. Analysis of AhR transcription

Understanding the effective interactions between AhR nuclear receptors and exogenous ligand contaminants was crucial for unraveling the molecular mechanisms that interfere with the biological effects of contaminants (Cui et al., 2022; Tan et al., 2020). In this study, the interactions of AhR LBD with pyrene and its derivatives were simulated using molecular docking and MD simulations to identify their molecular conformation of protein-ligand complexes, which leads to AhR transcriptional activation. Based on the docked complexes of AhR with pyrene and its derivatives, the optimal complex conformations with the

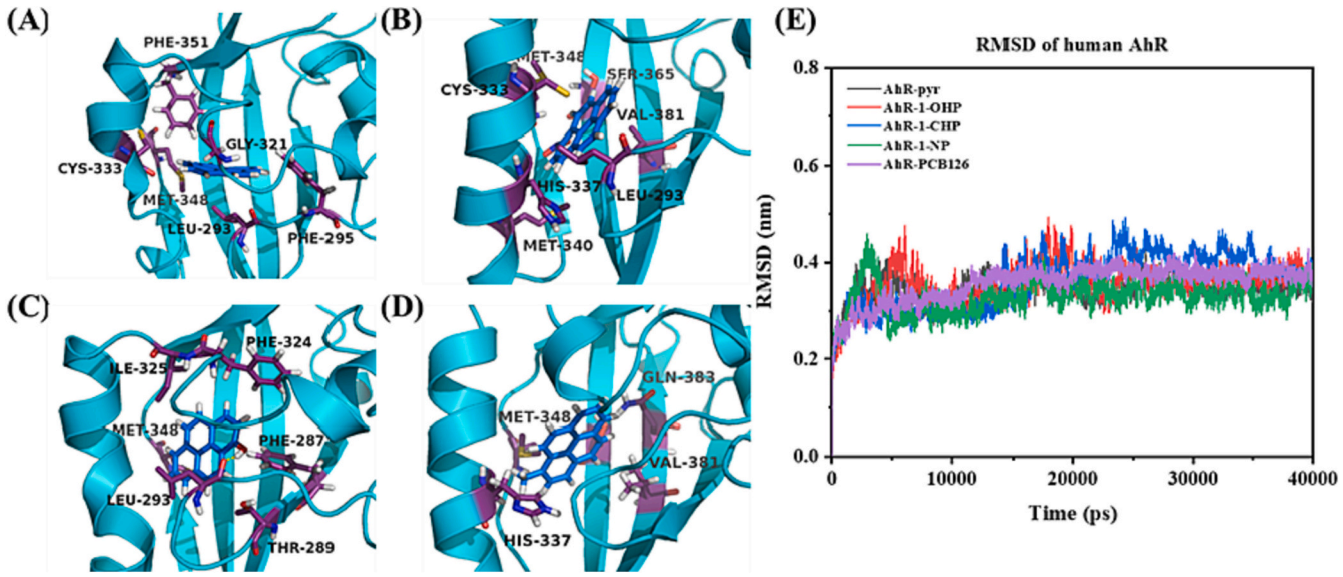

Fig. 5. Disrupting characteristics of pyrene and derivatives towards AhR. Binding modes of pyrene (A) and 1-nitropyrene (B) and 1-hydroxypyrene (C) and 1-methylpyrene (D) to AhR LBD. Amino acid residues within 2.5 Å of pyrene and derivatives are marked in purple, and the hydrogen bond formed is indicated by yellow dashed lines. (E) Comparison of the measured protein backbone RMSD from 40 ns MD simulations.

lowest binding energy were shown in Fig. S4, and they were selected as the initial structure for subsequent MD simulations. Statistical analysis of 40 ns snapshots of MD trajectories showed that pyrene derivatives were located in the binding cavity of AhR LBD, similar with the original pyrene (Fig. 5A-D). However, the different binding free energies (ΔG_{bind}) were obtained for pyrene and its derivatives to AhR. Seen from Table S1, the calculated ΔG_{bind} value of pyrene was −16.07 kcal/mol, higher than those of pyrene derivatives (−21.15 to −27.25 kcal/mol). These data indicate that pyrene derivatives could exhibit stronger affinity with AhR relative to original pyrene. Furthermore, this finding explained the abovementioned experimental results that pyrene derivatives could be more favorable activation of AhR transcription, resulting in more serious adverse effect on human health. As for the pyrene derivatives, 1-nitropyrene displayed the lowest binding energy at −27.25 kcal/mol, followed by 1-methylpyrene (−24.96 kcal/mol) and 1-hydroxypyrene (−21.25 kcal/mol). These data suggest that 1-nitropyrene has a relatively stronger binding interaction to human AhR, and further potentially impose more serious risks on human health relative to 1-methylpyrene and 1-hydroxypyrene.

The distinct binding modes of pyrene and its derivatives could lead to different conformational changes in AhR LBD. In addition to the binding energy, the stable conformation was more favorable for AhR transcription (Zhang et al., 2022a). The conformational changes of pyrene derivatives with the AhR protein backbone were analyzed through a 40 ns MD trajectory as illustrated in Fig. 5E. The RMSD of the AhR protein backbone reached equilibrium in 40 ns. The average RMSD of AhR bound by 1-nitropyrene was the smallest at 0.33 nm, lower than those of 1-hydroxypyrene (0.36 nm) and 1-methylpyrene (0.36 nm). This suggests that among the tested pyrene derivatives, the most stable conformation was displayed in the binding of AhR with 1-nitropyrene. That is, 1-nitropyrene could possess stronger AhR agonist activity *via* stabilize the AhR protein backbone, which is consistent with the observation that hydroxylated PCBs possessing AhR agonist activity stabilize the protein backbone (Cao et al., 2013). Taken together, our findings suggested that the low binding energy and stable conformation pyrene and its derivatives could initiate molecular initiation events leading to AhR activation, which may explain their adverse effects on lung. Pyrene derivatives especially 1-nitropyrene are stronger agonists than the parent pyrene.

3.5. Identification of key amino acid for AhR activation

Receptor conformation often be affected by interactions between agonists and amino acids, leading to signal transduction through ligand binding, recruitment of coregulators, and regulation of gene expression (Rosenfeld et al., 2006). Therefore, we analyzed the key amino acids of pyrene and its derivatives on AhR LBD, and calculated the E_{MM} of pyrene and its derivatives with all amino acid residues on human AhR, as shown in Fig. 6. The average E_{MM} value was −0.16 kcal/mol, and thus amino acid residues exhibiting an E_{MM} below −1.6 kcal/mol, were identified as critical in relation to pyrene and its derivatives, according to the identification method of amino acid residues between TCDD and AhR LBD (Zhang et al., 2018b). For pyrene, Leu293 (−2.66 kcal/mol) was identified as the key amino acid residue. However, in the case of pyrene derivatives, it was observed that the three different amino acid residues Cys333, Met348, and Val381 were identified as the crucial residues for 1-nitropyrene. They are also closely interacting residues in TCDD binding with AhR (Salzano et al., 2011). Among them, Cys333 had the highest E_{MM} (−2.33 kcal/mol), therefore, these three residues are reasonably considered to be important for 1-nitropyrene. Key amino acids residues in 1-hydroxypyrene were identified as Leu293 (−1.80 kcal/mol) and Phe287 (−1.77 kcal/mol), with Leu293 forming a hydrogen bond with 1-hydroxypyrene (Fig. 5C). The amino acid residues that form the H bond were important for the biological function of proteins (Tian et al., 2022), it showed that Leu293 played an important role in the activation of AhR by 1-hydroxypyrene. And Met348 (−2.11 kcal/mol) is a key residue affecting 1-methylpyrene, the significance of the amino acids has been reported previously (Cao et al., 2013). Overall, the type and number of amino acid residues can significantly affect the activation mechanism of AhR mediated by pyrene and its derivatives at the atomic level. The adverse lung effects of pyrene and its derivatives could be triggered *via* their binding to the active center of AhR and then interacting with amino acid residues of AhR. This can lead to alterations in AhR expression and downstream gene transcription, which may elicit further adverse effects at higher levels of biological tissues.

4. Conclusions

In this study, we investigated the lungs adverse effects of pyrene, 1-nitropyrene, 1-hydroxypyrene and 1-methylpyrene using *in vitro* and *in*

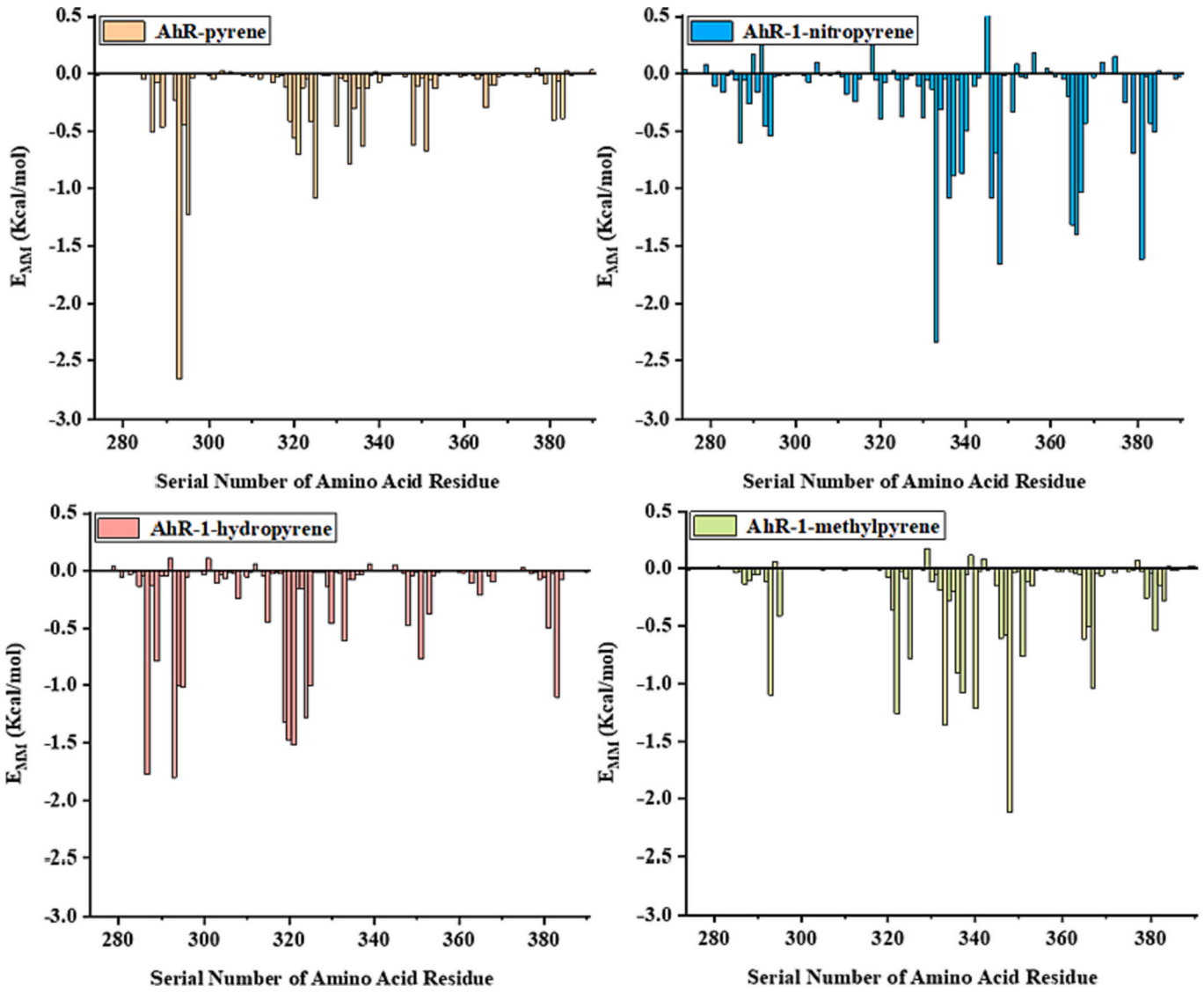

Fig. 6. The molecular mechanics energy between pyrene and its derivatives with amino acid residues in the ligand-binding domain (LBD) of AhR in human.

vivo methods. Western blot analysis revealed that pyrene had no significant effect on the expression of AhR protein, while 1-nitropyrene and 1-hydroxypyrene increased the expression of AhR protein by 2.0-fold and 1.2-fold, respectively. Furthermore, qPCR results demonstrated that exposure to pyrene, 1-hydroxypyrene, and 1-methylpyrene induced the expression of AhR and its downstream target genes CYP1A1 and CYP1B1 in lung cells. These findings suggested that 1-nitropyrene, 1-hydroxy-pyrene, and 1-methylpyrene had a more significant effect on interfering with AhR signals than pyrene. The binding energies of pyrene and its derivatives ranged from −16.07 to −27.25 kcal/mol by MD simulations. 1-nitropyrene was the lowest binding energy and the most stable conformation. Experimental and theoretical results confirmed that pyrene was identified as a weak agonist, whereas 1-nitropyrene, 1-hydroxypyrene and 1-methylpyrene exhibited greater agonistic activity than parent pyrene, resulting in adverse effects in this study. The essential reason for the difference in AhR activation between pyrene and its derivatives was explored from the atomic level, which was caused by the type and number of key amino acid residues of pyrene and its derivatives interacting with AhR. However, the occurrence of diseases is closely related to various proteins in the body, indicating that the reactions of pyrene and its three derivatives not only include direct binding with AhR, but also binding with other proteins. In our future research, we need to consider the mechanisms and influencing factors of other proteins to more comprehensively understand the impact of polycyclic aromatic hydrocarbons and their derivatives on human health.

CRediT authorship contribution statement

Mei Wang: Formal analysis, Methodology, Writing – original draft. **Na Luo:** Data curation, Formal analysis. **Yanpeng Gao:** Data curation, Methodology. **Guiying Li:** Writing – review & editing. **Taicheng An:** Conceptualization, Funding acquisition, Supervision.

Declaration of competing interest

The authors declare that they have no known competing financial interests or personal relationships that could have appeared to influence the work reported in this paper.

Data availability

No data was used for the research described in the article.

Acknowledgments

This work was financially supported by National Key Research and Development Project (2023YFC3905102 and 2019YFC1804503), and Guangdong Provincial Key R&D Program (2022-GDUT-A0007).

Appendix A. Supplementary data

Supplementary data to this article can be found online at https://doi.org/10.1016/j.scitotenv.2024.170030.

References

Abraham, M.J., Murtola, T., Schulz, R., Páll, S., Smith, J.C., Hess, B., Lindahl, E., 2015. GROMACS: high performance molecular simulations through multi-level parallelism from laptops to supercomputers. SoftwareX 1, 19–25.

Advanced Chemistry Development, 2016. ACD/Labs Percepta, Inc.,Toronto, Ontario, Canada.

Berge, G., Mollerup, S., S, O.V., Hewer, A., Phillips, D.H., Eilertsen, E., Haugen, A., 2004. Role of estrogen receptor in regulation of polycyclic aromatic hydrocarbon metabolic activation in lung. Lung Cancer 45, 289–297.

Bisson, W.H., Koch, D.C., O'Donnell, E.F., Khalil, S.M., Kerkvliet, N.I., Tanguay, R.L., Abagyan, R., Kolluri, S.K., 2009. Modeling of the aryl hydrocarbon receptor (AhR) ligand binding domain and its utility in virtual ligand screening to predict new AhR ligands. J. Med. Chem. 52, 5635–5641.

Brinchmann, B.C., Le Ferrec, E., Bisson, W.H., Podechard, N., Huitfeldt, H.S., Gallais, I., Sergent, O., Holme, J.A., Lagadic-Gossmann, D., Ovrevik, J., 2018. Evidence of selective activation of aryl hydrocarbon receptor nongenomic calcium signaling by pyrene. Biochem. Pharmacol. 158, 1–12.

Cao, F., Li, X., Ye, L., Xie, Y., Wang, X., Shi, W., Qian, X., Zhu, Y., Yu, H., 2013. Molecular docking, molecular dynamics simulation, and structure-based 3D-QSAR studies on the aryl hydrocarbon receptor agonistic activity of hydroxylated polychlorinated biphenyls. Environ. Toxicol. Pharmacol. 36, 626–635.

Chai, L., Zhang, H., Song, R., Yang, H., Yu, H., Paneth, P., Kepp, K.P., Akamatsu, M., Ji, L., 2021. Precision biotransformation of emerging pollutants by human cytochrome P450 using computational-experimental synergy: a case study of Tris (1,3-dichloro-2-propyl) phosphate. Environ. Sci. Technol. 55, 14037–14050.

Cui, S., Yu, Y., Zhan, T., Gao, Y., Zhang, J., Zhang, L., Ge, Z., Liu, W., Zhang, C., Zhuang, S., 2022. Carcinogenic Risk of 2,6-Di-tert-Butylphenol and Its Quinone Metabolite 2,6-DTBQ Through Their Interruption of RARbeta: In Vivo, In Vitro, and In Silico Investigations. Environ. Sci. Technol. 56, 480–490.

Doering, J.A., Farmahin, R., Wiseman, S., Beitel, S.C., Kennedy, S.W., Giesy, J.P., Hecker, M., 2015. Differences in activation of aryl hydrocarbon receptors of white sturgeon relative to lake sturgeon are predicted by identities of key amino acids in the ligand binding domain. Environ. Sci. Technol. 49, 4681–4689.

Dundas, J., Ouyang, Z., Tseng, J., Binkowski, A., Turpaz, Y., Liang, J., 2006. CASTp: computed atlas of surface topography of proteins with structural and topographical mapping of functionally annotated residues. Nucleic Acids Res. 34, 116–118.

Fang, J., Dong, S., Boogaard, P.J., Rietjens, I., Kamelia, L., 2022. Developmental toxicity testing of unsubstituted and methylated 4- and 5-ring polycyclic aromatic hydrocarbons using the zebrafish embryotoxicity test. Toxicol. In Vitro 80, 105312.

Freitas, F., Brucker, N., Durgante, J., Bubols, G., Bulcao, R., Moro, A., Charao, M., Baierle, M., Nascimento, S., Gauer, B., Sauer, E., Zimmer, M., Thiesen, F., Castro, I., Saldiva, P., Garcia, S.C., 2014. Urinary 1-hydroxypyrene is associated with oxidative stress and inflammatory biomarkers in acute myocardial infarction. Int. J. Environ. Res. Public Health 11, 9024–9037.

Frisch, M.J.T., G.W., Schlegel, H.B., Scuseria, G.E., Robb, M.A., Cheeseman, J.R., Scalmani, G., Barone, V., Mennucci, B., Petersson, G.A., Nakatsuji, M., Caricato, M., Li, X., Hratchian, H.P., Izmaylov, A.F., Bloino, J., Zheng, G., Sonnenberg, J.L., Hada, M., Ehara, M., Toyota, K., Fukuda, R., Hasegawa, J., Ishida, M., Nakajima . Y., T.H., Kitao, O., Nakai, H., Vreven, T., Montgomery, J.A.Jr., Peralta, J.E., Ogliaro, F., Bearpark, M., Heyd, J.J., Brothers, E., Kudin, K.N., Staroverov, V.N., Keith, T., Kobayashi, R., Normand, R., Raghavachari, K., Rendell, A., Burant, C., Iyengar, S.S., Tomasi, J., Cossi, M., Rega, N., Millam, J.M., Klene, M., Knox, J.E., Cross, J.B., Bakken, V., Adamo, C., Jaramillo, J., Gomperts, R., Stratmann, R.E., Martin, R.L., Morokuma, K., Zakrzewski, V.G., Voth, G.A., Salvador, P., Dannenberg, J.J., Dapprich, S., Daniels, A.D., Farkas, O., Foresman, J.B., Ortiz, J.V., Cioslowski, J., Fox, D.J., 2013. GAUSSIAN 09, Revision D.01, Guassian, Inc.: Wallingford CT.

Gao, R., Li, D., Yun, Y., Sang, N., 2019. Dysfunction of the hippo-yap pathway drives lung cancer metastasis induced by 1-nitropyrene through adhesion molecular activation. Environ. Sci. Technol. Lett. 6, 270–276.

Gao, Y., Hu, X., Deng, C., Wang, M., Niu, X., Luo, N., Ji, Y., Li, G., An, T., 2023. New insight into molecular mechanism of P450-catalyzed metabolism of emerging contaminants and its consequence for human health: a case study of preservative methylparaben. Environ. Int. 174, 107890.

Garrison, P.M., Tullis, K., Aarts, J.M., Brouwer, A., Giesy, J.P., Denison, M.S., 1996. Species-specific recombinant cell lines as bioassay systems for the detection of 2,3,7,8-tetrachlorodibenzo-p-dioxin-like chemicals. Fundam. Appl. Toxicol. 30, 194–203.

Gawlik, M., Trawinski, J., Skibinski, R., 2020. Identification and characterization of citalopram new metabolites with the use of UHPLC-Q-TOF technique: in silico toxicity assessment of the identified transformation products. J. Pharm. Biomed. Anal. 186, 113299.

Gysel, N., Dixit, P., Schmitz, D.A., Engling, G., Cho, A.K., Cocker, D.R., Karavalakis, G., 2018. Chemical speciation, including polycyclic aromatic hydrocarbons (PAHs), and toxicity of particles emitted from meat cooking operations. Sci. Total Environ. 633, 1429–1436.

Han, M., Kong, J., Yuan, J., He, H., Hu, J., Yang, S., Li, S., Zhang, L., Sun, C., 2019. Method development for simultaneous analyses of polycyclic aromatic hydrocarbons and their nitro-, oxy-, hydroxy- derivatives in sediments. Talanta 205, 120128.

Hayakawa, K., Tang, N., Toriba, A., Nagato, E.G., 2020. Calculating sources of combustion-derived particulates using 1-nitropyrene and pyrene as markers. Environ. Pollut. 265, 114730.

Hirano, M., Hwang, J.H., Park, H.J., Bak, S.M., Iwata, H., Kim, E.Y., 2015. In silico analysis of the interaction of avian aryl hydrocarbon receptors and dioxins to decipher isoform-, ligand-, and species-specific activations. Environ. Sci. Technol. 49, 3795–3804.

Hu, B., Tong, B., Xiang, Y., Li, S.R., Tan, Z.X., Xiang, H.X., Fu, L., Wang, H., Zhao, H., Xu, D.X., 2020. Acute 1-NP exposure induces inflammatory responses through activating various inflammatory signaling pathways in mouse lungs and human A549 cells. Ecotoxicol. Environ. Saf. 189, 109977.

Huang, B., Liu, M., Bi, X., Chaemfa, C., Ren, Z., Wang, X., Sheng, G., Fu, J., 2014. Phase distribution, sources and risk assessment of PAHs, NPAHs and OPAHs in a rural site of Pearl River Delta region, China. Atmos. Pollut. 5, 210–218.

Humphrey, W., Dalke, A., Schulten, K., 1996. VMD: visual molecular dynamics. J. Mol. Graph. 14 (33–38), 27–38.

Hwang, J.H., Kannan, K., Evans, T.J., Iwata, H., Kim, E.Y., 2020. Assessment of risks of dioxins for aryl hydrocarbon receptor-mediated effects in polar bear (Ursus maritimus) by in vitro and in silico approaches. Environ. Sci. Technol. 54, 1770–1781.

Idowu, O., Semple, K.T., Ramadass, K., O'Connor, W., Hansbro, P., Thavamani, P., 2020. Analysis of polycyclic aromatic hydrocarbons (PAHs) and their polar derivatives in soils of an industrial heritage city of Australia. Sci. Total Environ. 699, 134303.

Jin, U.H., Park, H., Li, X., Davidson, L.A., Allred, C., Patil, B., Jayaprakasha, G., Orr, A.A., Mao, L., Chapkin, R.S., Jayaraman, A., Tamamis, P., Safe, S., 2018. Structure-dependent modulation of aryl hydrocarbon receptor-mediated activities by flavonoids. Toxicol. Sci. 164, 205–217.

Jin, R., Liu, G., Zhou, X., Zhang, Z., Lin, B., Liu, Y., Qi, Z., Zheng, M., 2023. Analysis of polycyclic aromatic hydrocarbon derivatives in environment. Trac-Trends in Anal. Chem. 160, 116942.

Kumari, R., Kumar, R., Open Source Drug Discovery, C, Lynn, A., 2014. g_mmpbsa–a GROMACS tool for high-throughput MM-PBSA calculations. J. Chem. Inf. Model. 54, 1951–1962.

Kuntal, B.K., Aparoy, P., Reddanna, P., 2010. EasyModeller: a graphical interface to MODELLER. BMC. Res. Notes 3, 226.

Li, X., Yang, H., Sun, H., Lu, R., Zhang, C., Gao, N., Meng, Q., Wu, S., Wang, S., Aschner, M., Wu, J., Tang, B., Gu, A., Kay, S.A., Chen, R., 2017. Taurine ameliorates particulate matter-induced emphysema by switching on mitochondrial NADH dehydrogenase genes. Proc. Natl. Acad. Sci. 114, E9655–E9664.

Li, B., Ma, L.X., Sun, S.J., Thapa, S., Lu, L., Wang, K., Qi, H., 2020. Polycyclic aromatic hydrocarbons and their nitro-derivatives in urban road dust across China: spatial variation, source apportionment, and health risk. Sci. Total Environ. 747, 141194.

Li, Y., Bai, X., Ren, Y., Gao, R., Ji, Y., Wang, Y., Li, H., 2022. PAHs and nitro-PAHs in urban Beijing from 2017 to 2018: Characteristics, sources, transformation mechanism and risk assessment. J. Hazard. Mater. 436.

Lille-Langoy, R., Jorgensen, K.B., Goksoyr, A., Pampanin, D.M., Sydnes, M.O., Karlsen, O. A., 2021. Substituted two- to five-ring polycyclic aromatic compounds are potent agonists of Atlantic cod (Gadus morhua) aryl hydrocarbon receptors Ahr1a and Ahr2a. Environ. Sci. Technol. 55, 15123–15135.

Luo, Y., Zhang, B., Geng, N., Sun, S., Song, X., Chen, J., Zhang, H., 2022. Insights into the hepatotoxicity of pyrene and 1-chloropyrene using an integrated approach of metabolomics and transcriptomics. Sci. Total Environ. 829, 154637.

Misaki, K., Takamura-Enya, T., Ogawa, H., Takamori, K., Yanagida, M., 2016. Tumour-promoting activity of polycyclic aromatic hydrocarbons and their oxygenated or nitrated derivatives. Mutagenesis 31, 205–213.

Mohammed, R., Zhang, Z.F., Jiang, C., Hu, Y.H., Liu, L.Y., Ma, W.L., Song, W.W., Nikolaev, A., Li, Y.F., 2021. Fate and occurrence of polycyclic aromatic hydrocarbons and their derivatives in water and sediment from Songhua River, Northeast China. Water 13 (9), 1196.

Morris, G.M., Huey, R., Lindstrom, W., Sanner, M.F., Belew, R.K., Goodsell, D.S., Olson, A.J., 2009. AutoDock4 and AutoDockTools4: automated docking with selective receptor flexibility. J. Comput. Chem. 30, 2785–2791.

Motorykin, O., Santiago-Delgado, L., Rohlman, D., Schrlau, J.E., Harper, B., Harris, S., Harding, A., Kile, M.L., Massey Simonich, S.L., 2015. Metabolism and excretion rates of parent and hydroxy-PAHs in urine collected after consumption of traditionally smoked salmon for Native American volunteers. Sci. Total Environ. 514, 170–177.

Mueller, A., Ulrich, N., Hollmann, J., Zapata Sanchez, C.E., Rolle-Kampczyk, U.E., von Bergen, M., 2019. Characterization of a multianalyte GC-MS/MS procedure for detecting and quantifying polycyclic aromatic hydrocarbons (PAHs) and PAH derivatives from air particulate matter for an improved risk assessment. Environ. Pollut. 255, 112967.

Pandini, A., Denison, M.S., Song, Y.J., Soshilov, A.A., Bonati, L., 2007. Structural and functional characterization of the aryl hydrocarbon receptor ligand binding domain by homology modeling and mutational analysis. Biochemistry 46, 696–708.

Rosenfeld, M.G., Lunyak, V.V., Glass, C.K., 2006. Sensors and signals: a coactivator/corepressor/epigenetic code for integrating signal-dependent programs of transcriptionaf response. Genes Dev. 20, 1405–1428.

Salzano, M., Marabotti, A., Milanesi, L., Facchiano, A., 2011. Human aryl-hydrocarbon receptor and its interaction with dioxin and physiological ligands investigated by molecular modelling and docking simulations. Biochem. Biophys. Res. Commun. 413, 176–181.

Shoots, J., Fraccalvieri, D., Franks, D.G., Denison, M.S., Hahn, M.E., Bonati, L., Powell, W.H., 2015. An aryl hydrocarbon receptor from the salamander Ambystoma mexicanum exhibits low sensitivity to 2,3,7,8-Tetrachlorodibenzo-p-dioxin. Environ. Sci. Technol. 49, 6993–7001.

Sun, Y., Miller 3rd, C.A., Wiese, T.E., Blake, D.A., 2014. Methylated phenanthrenes are more potent than phenanthrene in a bioassay of human aryl hydrocarbon receptor (AhR) signaling. Environ. Toxicol. Chem. 33, 2363–2367.

Tan, H., Wang, X., Hong, H., Benfenati, E., Giesy, J.P., Gini, G.C., Kusko, R., Zhang, X., Yu, H., Shi, W., 2020. Structures of endocrine-disrupting chemicals determine binding to and activation of the estrogen receptor alpha and androgen receptor. Environ. Sci. Technol. 54, 11424–11433.

Tian, S., Yan, S., Meng, Z., Sun, W., Yan, J., Huang, S., Wang, Y., Zhou, Z., Diao, J., Li, L., Zhu, W., 2022. Widening the lens on prothioconazole and its metabolite prothioconazole-desthio: aryl hydrocarbon receptor-mediated reproductive disorders through *in vivo*, *in vitro*, and *in silico* studies. Environ. Sci. Technol. 56, 17890–17901.

Tomaz, S., Shahpoury, P., Jaffrezo, J.L., Lammel, G., Perraudin, E., Villenave, E., Albinet, A., 2016. One-year study of polycyclic aromatic compounds at an urban site in Grenoble (France): seasonal variations, gas/particle partitioning and cancer risk estimation. Sci. Total Environ. 565, 1071–1083.

Vondracek, J., Pencikova, K., Neca, J., Ciganek, M., Grycova, A., Dvorak, Z., Machala, M., 2017. Assessment of the aryl hydrocarbon receptor-mediated activities of polycyclic aromatic hydrocarbons in a human cell-based reporter gene assay. Environ. Pollut. 220, 307–316.

Vondracek, J., Pencikova, K., Ciganek, M., Pivnicka, J., Karasova, M., Hyzdalova, M., Strapacova, S., Palkova, L., Neca, J., Matthews, J., Lom, M.V., Topinka, J., Milcova, A., Machala, M., 2020. Environmental six-ring polycyclic aromatic hydrocarbons are potent inducers of the AhR-dependent signaling in human cells. Environ. Pollut. 266, 115125.

Wang, Y., Wang, Q., Wu, B., Li, Y., Lu, G., 2013. Correlation between TCDD acute toxicity and aryl hydrocarbon receptor structure for different mammals. Ecotoxicol. Environ. Saf. 89, 84–88.

Wiederstein, M., Sippl, M.J., 2007. ProSA-web: interactive web service for the recognition of errors in three-dimensional structures of proteins. Nucleic Acids Res. 35, W407–W410.

Zhang, L., Jin, Y., Han, Z., Liu, H., Shi, L., Hua, X., Doering, J.A., Tang, S., Giesy, J.P., Yu, H., 2018a. Integrated in silico and in vivo approaches to investigate effects of BDE-99 mediated by the nuclear receptors on developing zebrafish. Environ. Toxicol. Chem. 37, 780–787.

Zhang, R., Wang, X., Zhang, X., Song, C., Letcher, R.J., Liu, C., 2018b. Polychlorinated diphenylsulfides activate aryl hydrocarbon receptor 2 in zebrafish embryos: potential mechanism of developmental toxicity. Environ. Sci. Technol. 52, 4402–4412.

Zhang, J., Cui, S., Shen, L., Gao, Y., Liu, W., Zhang, C., Zhuang, S., 2022a. Promotion of bladder cancer cell metastasis by 2-Mercaptobenzothiazole via its activation of aryl hydrocarbon receptor transcription: molecular dynamics simulations, cell-based assays, and machine learning-driven prediction. Environ. Sci. Technol. 56, 13254–13263.

Zhang, Z.F., Chen, J.C., Zhao, Y.X., Wang, L., Teng, Y.Q., Cai, M.H., Zhao, Y.H., Nikolaev, A., Li, Y.F., 2022b. Determination of 123 polycyclic aromatic hydrocarbons and their derivatives in atmospheric samples. Chemosphere 296, 134025.

Zhou, J., Zhang, X., Li, Y., Feng, S., Zhang, Q., Wang, W., 2022. Endocrine-disrupting metabolic activation of 2-nitrofluorene catalyzed by human cytochrome P450 1A1: a QM/MM approach. Environ. Int. 166, 107355.